Structural and Electronic Properties of Defect-Free and Defect-Containing Polypropylene: A Computational Study by van der Waals Density-Functional Method

Huy-Viet Nguyen and Thinh H. Pham*

This paper presents a study on structural and electronic properties of bulk polypropylene – one of the fastest growing engineering plastics – based on density-functional calculations. The use of recently developed non-local van der Waals functionals to approximate the exchange–correlation energy is crucial for a good description of structural properties. Various types of chemical imperfections, their impacts on electronic properties of polypropylene are also studied.

1. Introduction

As a result of its low density, high melt point, tensile strength, and resistance to chemical attack, polypropylene (PP) has wide applications in both industrial and domestic products.[1] In particular, polypropylene is the polymer most widely used to manufacture capacitor film.[2] Increasing the energy density of high voltage capacitors requires further improvements in the electrical performance of the polypropylene capacitor film, especially improved dielectric breakdown field,[3] which motivates the present computational study on structural and electrical properties of this important polymeric material by means of computational quantum mechanics based on density-functional theory.

The engineering breakdown field of polypropylene is believed to be extrinsic.[3] Extrinsic factors that can affect breakdown strength of polypropylene include morphology[4] and chemical impurities.[3,5] Recent studies based on density-functional calculations have shown the presence of impurity states in the bandgap caused by chemical impurities in polyethylene[6] and polypropylene,[7] which may result in overlapping of the electron density between polymer backbones. This facilitates the hopping of charge carriers between valence and conduction bands, which increases the conductivity of the material and facilitates the thermal breakdown thereof.[5]

In this paper, we present a thorough study of structural and electronic properties of crystalline isotactic polypropylene (iPP) in the *α*-phase, i.e., monoclinic crystal structure[7] (**Figure 1**), both free of chemical defects and in the presence of chemical defects. This work addresses several shortcomings of the first computational study of polypropylene, namely the lack of long-range van der Waals interaction in the standard generalized gradient approximation (GGA) functionals as well as the inability of such computations to describe correctly the bandgap of the material. The applications of recently developed advanced functionals such as van der Waals density functionals[8,9] (vdW-DF) and hybrid functionals[10,11] address these issues. We also extend the previous study to consider the effect of additional chemical defects, such as conjugated double bonds, vinyl and dienone defects.

2. Computational Details

Our density-functional calculations were performed using the PWSCF code of the Quantum ESPRESSO distribution[12] which employs plane-wave pseudopotentials to solve the single-particle Kohn–Sham equations. In principle, density functional theory (DFT) is exact for the ground state of an interacting electron system, but in practice, approximations must be used for the so-called exchange–correlation (xc) energy which contains the quantum effect of electron–electron interactions. For polymeric systems, the use of standard local or semilocal functionals (such as, for instance, LDA, PBE, PW91) to approximate the xc energy does not predict structural properties with high fidelity because long-range interaction forces between polymer chains are not treated properly in these types of functionals. As a result, lattice constants along the inter-chain directions in polymer crystals are usually underestimated (overestimated) when local functional (semilocal functionals) are employed.[13] Although the use of dispersion-corrected functionals in which the long-range vdW interaction energy between atoms is added empirically to the total DFT energy improves the accuracy of LDA/GGA DFT computations,[13] a systematic study of structural properties of ten polymeric crystals[14] by the recently developed vdW-DF and its variants provided improved agreement with experiments. The

Dr. H.-V. Nguyen
Institute of Research and Development, Duy Tan University, K7/25 Quang Trung, Danang, Vietnam
E-mail: hviet.nguyen@gmail.com

Dr. H.-V. Nguyen
Institute of Physics, Vietnam Academy of Science and Technology, 18 Hoang Quoc Viet, Cau Giay, Hanoi, Vietnam

Dr. T. H. Pham
School of Electrical Engineering, Hanoi University of Science and Technology, 1 Dai Co Viet, Hai Ba Trung, Hanoi, Vietnam

DOI: 10.1002/pssb.201700036

 © 2017 WILEY-VCH Verlag GmbH & Co. KGaA, Weinheim

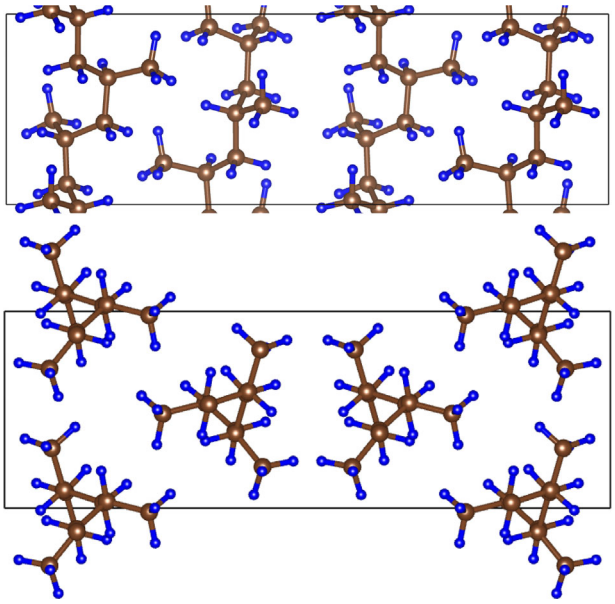

Figure 1. Ball-and-stick atomic model of isotactic polypropylene crystal (iPP) in the α-phase. C atoms are represented by bigger dark spheres, while the smaller ones are H atoms. The upper panel is the side view and the lower one is the top view.

latter has the advantage that the vdW interaction is incorporated naturally in the functionals.

In this study, we employed the vdW-DF approach to study structural properties of polypropylene crystals that are defect-free and that contain chemical defects. All pseudopotentials used in our calculations were generated using the PBE xc-functional in the Vanderbilt's ultrasoft framework as published in the GBRV pseudopotential library.[15] Optimized lattice constants are obtained using an automated optimization process in which the atomic positions and the size and shape of unit cell are allowed to change in such a way that the forces acting on each atom and the stress tensors are reduced in each step of the optimization process. This iterative process is terminated when the components of the forces acting on each atom are less than 10^{-4} Ry/bohr, and the total energy difference between successive steps is less than 10^{-7} Ry. These tight convergence thresholds were used to ensure good convergence of structural optimizations. Rather high cutoffs of plane waves used to represent the wavefunctions and charge density – 55 Ry for the former and 550 Ry for the latter – were used for the same reason. Brillouin zone sampling was performed using a $1 \times 3 \times 3$ k-point mesh generated automatically by the Monkhorst–Pack scheme.

Although the automated optimization process is efficient in predicting equilibrium lattice constants, especially for non-cubic crystals, the resulting lattice constants are not guaranteed to represent the global minimum of the potential energy surface. The automated optimization process can be trapped in a local minimum, especially for a complex system such as polypropylene. To reduce the uncertainty, we duplicated the procedure from four differing atomic configurations which were constructed by varying the lattice parameters randomly within 10% of experimental values.

The use of vdW-DFs does not address fully the so-called "bandgap problem," namely the underestimation of the calculated bandgap of semi-conducting and insulating materials relative to experimental data. This is also the case (see later) for the polypropylene studied in this work. The development of the so-called hybrid functionals,[10,11] for which part of Hartree–Fock (HF) exchange energy is mixed with the DFT exchange–correlation energy, improves the accuracy of the computed bandgap substantially. Therefore we also employ hybrid functionals in this study to improve the accuracy of electronic energy levels.

3. Results and Discussion

3.1. Lattice Constants of Defect-Free Crystalline Polypropylene

Lattice constants of the polypropylene crystal were calculated using the vdW-DF by Dion et al.[8] and its refinement named vdW-DF2 by Lee et al.,[9] as well as other variants, including DF-C09 by Cooper,[16] DF-optB88 and DF-optB86b by Klimeš et al.,[17] revDF2 by Hamada,[18] and rVV10 by Sabatini et al.[19] which is a revised version of VV10 functional by Vydrov and van Voorhis.[20] **Table 1** shows the calculated data of the lattice constants a, b, and c (c along the polymer chains) and the unit cell angle, β. Experimental values[21] are also shown for reference. Percent relative error of the lattice constants and the unit cell angle is plotted in **Figure 2**.

Table 1 and Figure 2 indicate that a- and b-lattice constants are overestimated greatly by the semilocal PBE functional, with relative errors of 10 and 7%, respectively, whereas the c-lattice constant is very close to the experimental value of 6.50 ± 0.05 Å. The unit cell angle is also off by about 3%. This is to be expected because C—C bonds along the polymer chains are strong covalent while the interaction between chains is determined by weak dispersion forces. Semilocal functionals, such as PBE, describe well the former but fail to capture the physics of the

Table 1. Lattice constants (c along the polymer chains) and unit cell angle of polypropylene crystal obtained using the standard semilocal PBE functional and several vdW functionals. Experimental values are included for comparison.

Method	a (Å)	b (Å)	c (Å)	β (°)
expt	20.78 ± 0.15	6.65 ± 0.05	6.50 ± 0.05	99.2
PBE	22.92	7.13	6.53	96.7
vdW-DF	20.65	6.77	6.58	98.7
DF-C09	19.20	6.54	6.47	99.4
DF-optB88	19.47	6.56	6.51	99.3
DF-optB86	19.55	6.58	6.50	99.2
vdW-DF2	19.98	6.62	6.58	99.1
revDF2	19.61	6.62	6.49	99.2
rVV10	19.26	6.52	6.50	99.7

© 2017 WILEY-VCH Verlag GmbH & Co. KGaA, Weinheim

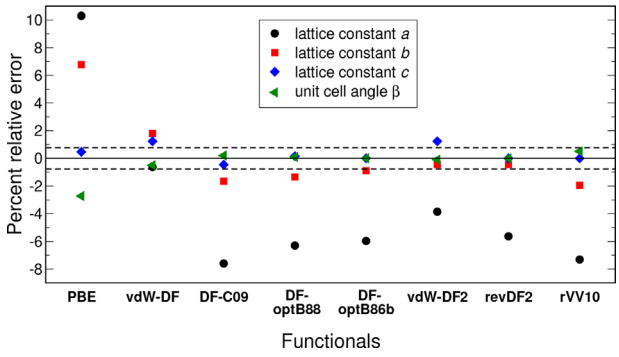

Figure 2. Percent relative errors of *a*, *b*, *c*-lattice constants (red squares, black circles, and blue diamonds, respectively) and the unit cell angle (green triangles) calculated using various functionals. The two dashed lines indicate the greatest error of the experimental lattice constants (error bars of all three lattice constants are all around 0.75%).

latter. On this basis, we suspect that the good agreement with experiments of the calculated results reported in Ref. [7] is fortuitous, possibly based on the choice of the initial configuration in the optimization process.

Errors in the computed *a*- and *b*-lattice constants should reduce when vdW density functionals are employed. This is indeed the case as shown in Figure 2 where the largest error in *b* is only 2% for a range of vdW functionals. The error bars for *a*-lattice constant also decrease, but not as much as that of *b*, except for the case of the original vdW-DF. The unit cell angles are also in better agreement with experiment. For the *c*-lattice constant, only vdW-DF and vdW-DF2 are less accurate than PBE, but the differences from the experimental value are only marginally greater than the uncertainty of experimental data.

In general, vdW-DF gives the most reasonable lattice constants and unit cell angle relative to experimental data. Therefore we employ this functional to study electronic properties of both defect-free and defect-containing polypropylene.

3.2. Electronic Band Structure of Defect-Free iPP

Electronic band structure and the density of states (DOS) of defect-free polypropylene calculated using vdW-DF functional are plotted in **Figure 3**. Based on these data, the use of vdW-DF improves prediction of structural properties significantly, but has little effect on the predicted electronic band structure compared to the semilocal functional. In particular, the calculated bandgap of about 6.1 eV is similar to the value of 6.3 eV computed using semilocal functional[7] and both underestimate the experimental value of 8.2 eV[22] by about 25%. This error stems from the fact that the functional derivatives of total energy with respect to the particle number calculated using local or semilocal functionals and vdW-DFs do not fulfill the discontinuity requirement at the integer values of the particle number.[23]

Although a rigorous and much more computationally demanding formulation of quasi-particle properties within a Green's function approach,[24] especially in the so-called *GW* approximation,[25] has become a popular tool for studying electronic excitations, it is too time-consuming to apply to study polypropylene. We therefore employ the more practical approach of using the hybrid functionals in which a fraction of the HF exchange is mixed with DFT exchange functionals. We have selected three popular hybrid functionals, namely PBE0[26] and B3LYP[10] which contain 25 and 20% of the HF exchange, respectively, and the range-separated HSE06 functional.[11] These hybrid-functional calculations are applied to the vdW-DF-optimized structure which produce a much improved computation of bandgap, with the direct bandgaps of 8.2, 7.8, and 7.5 eV for PBE0, B3LYP, and HSE06, respectively.

3.3. Electronic Properties of Defect-Containing iPP

We considered six types of defects placed in the main body of the polymer chain as shown schematically in the insets of Figure 5. A *double bond* defect (—CH_2CH_2—) is formed when one H atom

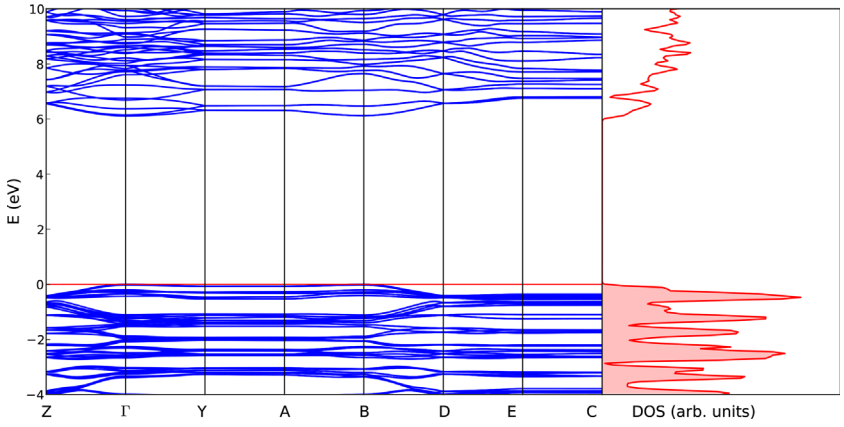

Figure 3. Electronic band structures and the density of states (DOS) of defect-free polypropylene calculated using vdW-DF functional. Band dispersions are drawn along the lines connecting the following special points in the first Brillouin zone: Z(0, 0, 1/2), Γ(0, 0, 0), Y(0, 1/2, 0), A(1/2, 1/2, 0), B(1/2, 0, 0), D(1/2, 0, 1/2), E(1/2, 1/2, 1/2), and C(0, 1/2, 1/2). The zero-energy level was set to the top of valence band.

© 2017 WILEY-VCH Verlag GmbH & Co. KGaA, Weinheim

is removed from each of two adjacent C atoms. When the H atom in a C—H bond is replaced by an —OH group, a *hydroxyl* defect is created. *Carbonyl* (C═O) and *vinyl* defects are formed when two C—H bonds of a C atom are replaced by a double bond with an O atom and a $=CH_2$ group, respectively. *Conjugated double bonds* ($-CH_2=CH-CH=CH_2-$) form where single C—C bond occurs between two double bond defects. *Dienone* ($-CH_2=CH-CH=O$) is the combination of a double bond and a carbonyl defect. These types of defects typically occur in polyethylene (PE), in which context they have been studied both computationally and experimentally.[27] Given the similar nature of chemical bonds in PE and PP, these types of defects are likely to occur in PP.

With the presence of defects, the geometry optimization procedure should be applied to find the lattice constants of defect-containing iPP. However, one might expect that the unit cell of defect-containing iPP does not differ greatly from that of defect-free iPP because the latter is already quite large. Computed data for a carbonyl defect with the vdW-DF functional indicate that the unit cell is nearly monoclinic, with three lattice vectors of 20.37, 6.86, and 6.58 Å. Since the differences between these lattice constants and those of defect-free iPP unit cell are small, we use a simple procedure to determine the optimized structures of defect-containing iPP based on fixing the unit cell and relaxing only the atoms in the cell. We have verified for carbonyl that this simple procedure does not result in significant changes to the local atomic structure of the defect or the computed electronic properties. For instance, the lengths of C═O double bond are 1.226 Å for both cases, while the C—C single bonds at and away from the defect are almost the same (1.552 vs. 1.551 Å and 1.549 vs. 1.548 Å). The differences in O—C—C and C—C—C angles for two structures are only a fraction of degree. **Figure 4** also shows that there is practically no difference between the DOS of two structures. We have therefore applied the simple optimization method to find the equilibrium structures for all other types of defects in this study.

Although all chemical defects considered in this work are located in the main body of the polymer chain, several configurations are possible for each defect type. As can be seen in the side view in Figure 1, a unit cell contains six C atoms in the main body of each polymer chain. Among these six C atoms, three make C—H bonds with two H atoms while for each of other three C atoms, a C—H bond is replaced by a C—C bond with CH_3 group. As a result, six configurations are possible for double bond and conjugated double bond defects (2 and 4 H atoms are removed from 2 and 4 adjacent C atoms, respectively) while only three possible configurations are available for carbonyl defects (two C—H bonds of one C atom are replace by a C═O double bond). We have compared the total energies of the various configurations for these three defects and found that the largest energy differences among possible locations are 0.39, 0.08, and 0.05 eV per unit cell for conjugated double bond, double bond, and carbonyl defects, respectively. Given that the iPP unit cell contains 36 C atoms and about 70 H atoms, determining definitively the most energetically favorable configuration based on these small energy differences is not possible. Therefore in the study of electronic properties of defect-containing iPP presented below, the atomic configuration used in the calculations is chosen arbitrarily from possible configurations for each defect type.

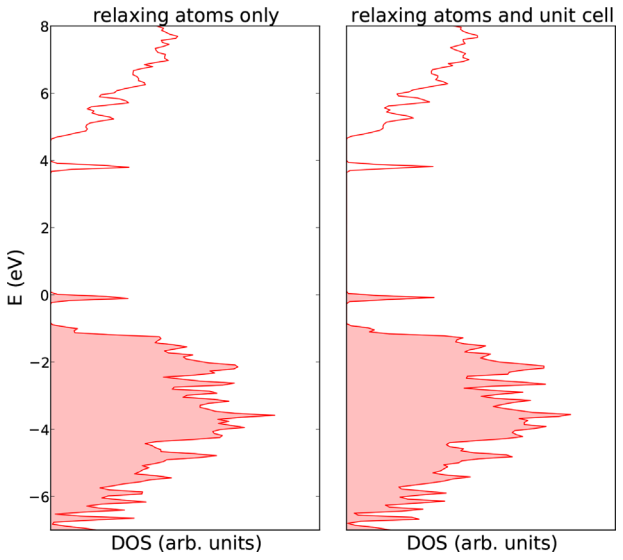

Figure 4. The DOS of iPP with a carbonyl defect placed in the main body of the polymer chain. On the left: DOS obtained using a simple geometry optimization procedure where the unit cell is fixed as that of defect-free iPP and only atoms in the cell are relaxed. On the right: DOS of fully optimized structure where both atoms and the size and shape of unit cell are allowed to change.

While the inclusion of van der Waals interaction has important impact in describing the lattice parameters of iPP crystal, its effect on the local atomic structure of defects is insignificant as a result of the covalent nature of defect chemical bonds considered in this work. This is the case for all defects as seen from **Table 2**, namely the lengths of C═C double bonds and C—O bonds calculated using the vdW-DF functional are nearly identical to the values obtained using the PBE functional. This is a necessary feature of any successful vdW functionals.

To consider the impact of these chemical defects on electronic structure of iPP, we have performed DOS calculations employing the vdW-DF functional for defect-containing iPP with the six

Table 2. The lengths of C═C double bonds and C—O bonds of defects considered in this work calculated using PBE and vdW-DF functionals.

	C═C (Å)		C—O (Å)	
Defects	PBE	vdW-DF	PBE	vdW-DF
Double bond	1.353	1.353	–	–
Hydroxyl	–	–	1.444	1.460
Carbonyl	–	–	1.225	1.226
Vinyl	1.342	1.340	–	–
Conj. double bond	1.360	1.350	–	–
	1.359	1.352	–	–
Dienone	1.354	1.354	1.233	1.235

© 2017 WILEY-VCH Verlag GmbH & Co. KGaA, Weinheim

chemical defects mentioned above. Resulting data are plotted in the top row of **Figure 5**, together with molecular structure in the inset showing the positions of defects. Our calculation results for the double bond, hydroxyl, and carbonyl defects are in qualitative agreement with those reported in Ref. [7] which were obtained using a GGA functional. This is not unexpected as the vdW-DF functional, while better than GGA in computing structural properties, still suffers from the bandgap problem, including the description of defect levels, as do local and semilocal functionals. Among the six defects studied, the carbonyl, conjugated double bonds, and dienone cause well-defined occupied and unoccupied states in the bandgap which can trap electrons and holes. Thus, these defects have the most significant impact on electronic properties of iPP, including the reduction of dielectric breakdown field.

To explore the origin as well as the character of these defect states, partial charge densities of the lowest unoccupied and highest occupied states were visualized, as shown in the middle and bottom rows of Figure 5, respectively. All occupied defect states are localized with σ-type interaction between C atoms in C═C double bonds and between C and O atoms in C—O bonds. For defects with well-defined unoccupied states in the gap, i.e., carbonyl, vinyl, conjugated double bond, and dienone, the defect orbitals are also localized in the defect region but with π-type interaction between atoms. As shown in the DOS plots, unoccupied defect states for the case of double bond and

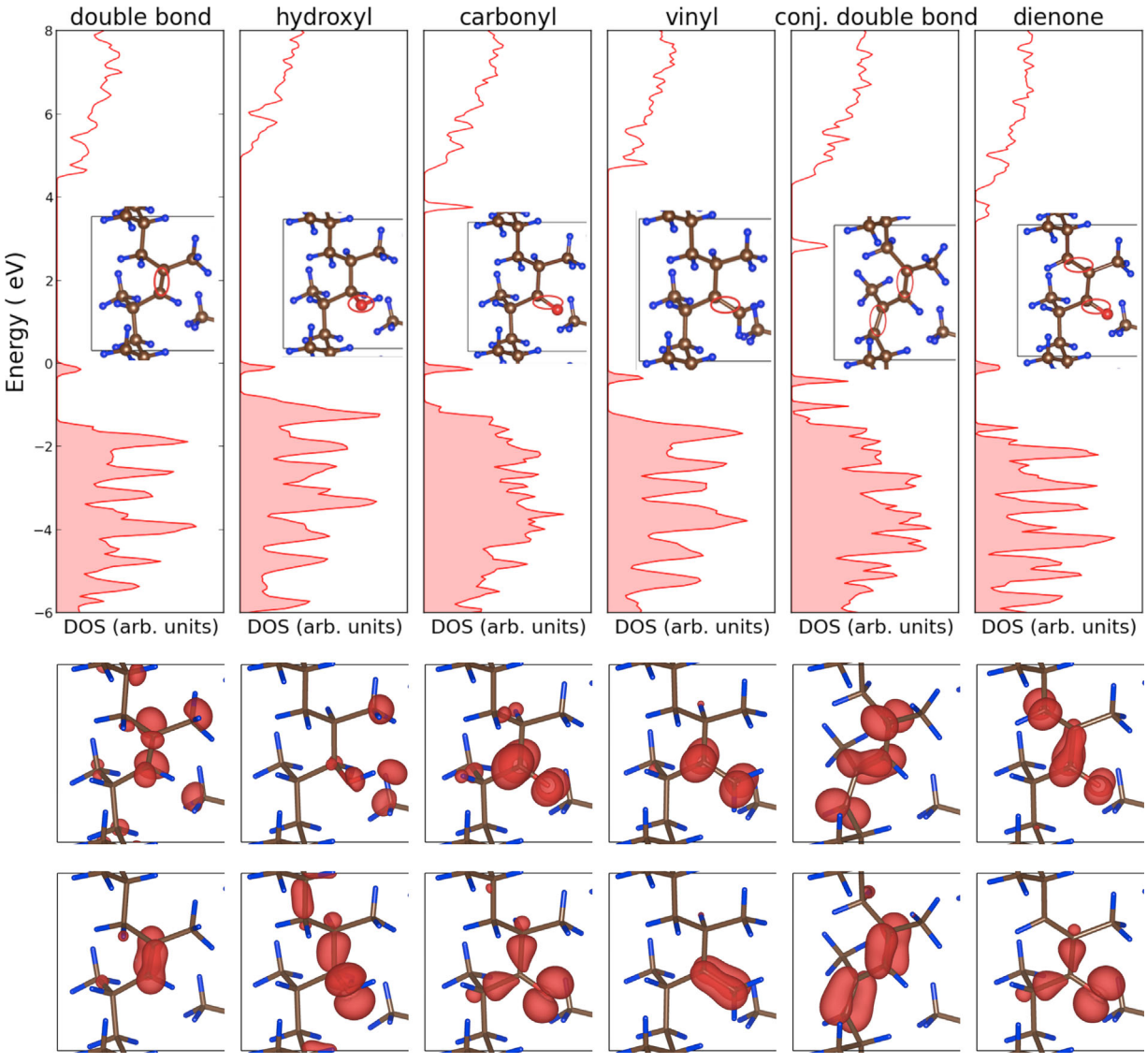

Figure 5. Top row: the DOS of defect-containing iPP with six types of chemical defects placed in the main body of the polymer chain calculated using vdW-DF functional. The insets show schematics of defect positions in ball-and-stick atomic representations where C, H, and O atoms are indicated by gray, blue, and red balls, respectively. Middle row: isosurfaces of the lowest unoccupied state partial charge densities for all defects. Bottom row: the same as the middle row but for the highest occupied states.

© 2017 WILEY-VCH Verlag GmbH & Co. KGaA, Weinheim

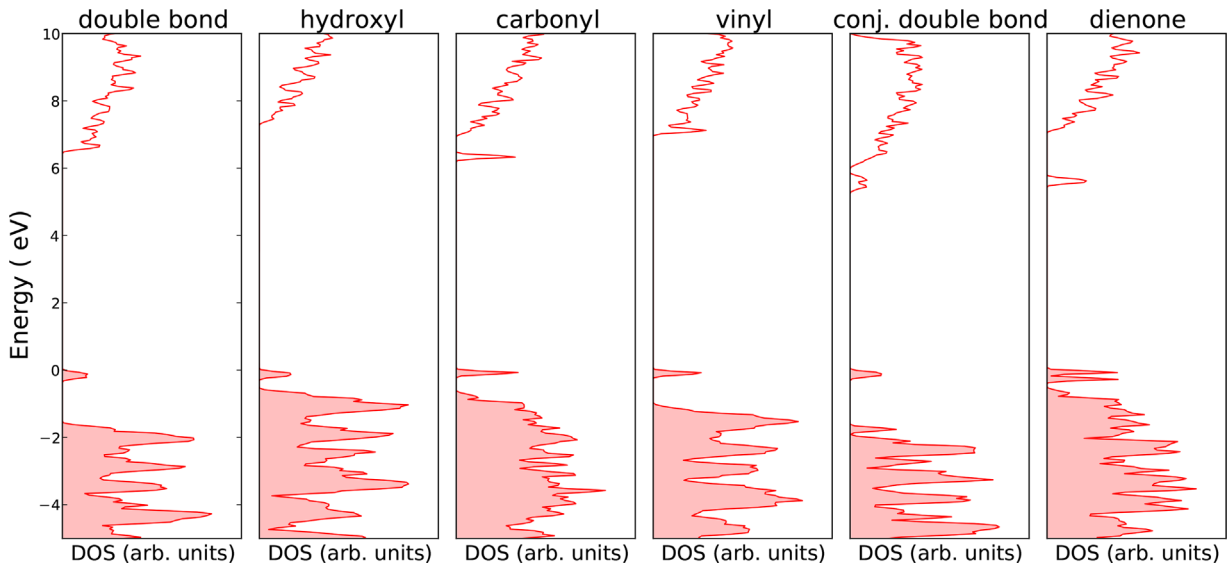

Figure 6. The DOS of defect-containing iPP with six types of chemical defects calculated using the hybrid functional PBE0.

hydroxyl are mixed with the conduction states and, as a result, partial charge densities of the lowest unoccupied states are more delocalized and do not show a π-type interaction as clear as the other cases.

The effect of hybrid functionals on defect energy levels is investigated by computing the DOS of defect-containing iPP for all six types of chemical defects using the PBE0 functional. The resulting data are presented in **Figure 6** which shows a qualitatively similar picture to the one obtained using the vdW-DF functional. Well-defined occupied and unoccupied states still occur for the case of carbonyl, vinyl, conjugated double bonds, and dienone defects, but they are separated by about 5–6 eV as the result of larger (and closer relative to the experimental values) bandgap prediction of hybrid functionals.

4. Summary

In this work, we have performed DFT calculations to study the structural and electronic properties of defect-free iPP and iPP that contains chemical defects. Our study shows that, as for other polymeric crystals, correct computation of the equilibrium structure of iPP requires the inclusion of long range van der Waals interaction, e.g., by using van der Waals density functionals, rather than local or semilocal functionals. vdW functionals do not improve the underestimation of bandgap for which hybrid functionals are necessary. Calculations of iPP with six chemical defects indicate well-defined occupied, and in some cases, unoccupied levels in the bandgap, most significantly for carbonyl, conjugated double bond, and dienone defects. This result partly explains for the reduction of dielectric breakdown strength of polypropylene material in practice. Our study thus provides useful information for further investigations of more complex electrical processes, e.g., dielectric breakdown, in this material by first-principles DFT calculations.

Acknowledgements

This research is funded by Vietnam National Foundation for Science and Technology Development (NAFOSTED) under Grant No. 103.99-2012.68. We would like to thank Dr. Steven A. Boggs at NonLinear Systems, Inc. for proof reading and helpful comments on our manuscript and an anonymous reviewer for useful suggestions that helped to improve our work. One of the author (HVN) would like to acknowledge the Abdus Salam International Centre for Theoretical Physics where part of this work was done during a visit under the Associate Programme.

Conflict of Interest

The authors declare no conflict of interest.

Keywords

chemical defects, DFT calculations, polypropylene, van der Waals density functionals

Received: January 21, 2017
Revised: September 11, 2017
Published online:

[1] E. P. Moore, *Polypropylene Handbook*, Hanser-Gardner Publications, Cincinnati, OH **1996**.
[2] J. Ho, R. Ramprasad, S. Boggs, *IEEE Trans. Dielectr. Electr. Insul.* **2007**, *14*, 5.
[3] T. D. Huan, S. Boggs, G. Teyssedre, C. Laurent, M. Cakmak, S. Kumar, R. Ramprasad, *Prog. Mater. Sci.* **2016**, *83*, 236.
[4] L. Y. Gao, D. M. Tu, S. C. Zhou, Z. L. Zhang, *IEEE Trans. Electr. Insul.* **1990**, *25*, 535.
[5] L. A. Dissado, J. C. Fothergill, *Electrical Degradation and Breakdown in Polymers*, IEE Materials and Devices Series, Vol. 9, Peter Peregrinus, London **1992**.
[6] A. Huzayyin, S. Boggs, R. Ramprasad, *IEEE Trans. Dielectr. Electr. Insul.* **2010**, *17*, 3.

 © 2017 WILEY-VCH Verlag GmbH & Co. KGaA, Weinheim

[7] M. E. Stournara, R. Ramprasad, *J. Mater. Sci*. **2010**, *45*, 443.
[8] M. Dion, H. Rydberg, E. Schröder, D. C. Langreth, B. I. Lundqvist, *Phys. Rev. Lett*. **2004**, *92*, 246401.
[9] K. Lee, E. D. Murray, L. Kong, B. I. Lundqvist, D. C. Langreth, *Phys. Rev. B* **2010**, *82*, 081101.
[10] A. D. Becke, *J. Chem. Phys*. **1993**, *98*, 1372.
[11] J. Heyd, G. E. Scuseria, M. Ernzerhof, *J. Chem. Phys*. **2003**, *118*, 8207.
[12] P. Giannozzi, S. Baroni, N. Bonini, M. Calandra, R. Car, C. Cavazzoni, D. Ceresoli, G. L. Chiarotti, M. Cococcioni, I. Dabo, A. Dal Corso, S. de Gironcoli, S. Fabris, G. Fratesi, R. Gebauer, U. Gerstmann, C. Gougoussis, A. Kokalj, M. Lazzeri, L. Martin-Samos, N. Marzari, F. Mauri, R. Mazzarello, S. Paolini, A. Pasquarello, L. Paulatto, C. Sbraccia, S. Scandolo, G. Sclauzero, A. P. Seitsonen, A. Smogunov, P. Umari, R. M. Wentzcovitch, *J. Phys.: Condens. Matter* **2009**, *39*, 395502.
[13] C.-S. Liu, G. Pilania, C. Wang, R. Ramprasad, *J. Phys. Chem. A* **2012**, *116*, 9347.
[14] T. H. Pham, R. Ramprasad, H.-V. Nguyen, *J. Chem. Phys*. **2016**, *144*, 214905.
[15] K. F. Garrity, J. W. Bennett, K. M. Rabe, D. Vanderbilt, *Comput. Mater. Sci*. **2014**, *81*, 446.
[16] V. R. Cooper, *Phys. Rev. B* **2010**, *81*, 161104(R).
[17] J. Klimeš, D. R. Bowler, A. Michaelides, *J. Phys.: Condens. Matter* **2010**, *22*, 022201; *Phys. Rev. B* **2011**, *83*, 195131.
[18] I. Hamada, *Phys. Rev. B* **2014**, *89*, 121103(R).
[19] R. Sabatini, T. Gorni, S. de Gironcoli, *Phys. Rev. B* **2013**, *87*, 041108(R).
[20] O. A. Vydrov, T. Van Voorhis, *J. Chem. Phys*. **2010**, *133*, 244103.
[21] G. Natta, P. Corradini, *Nuovo Cimento Suppl*. **1960**, *15*, 40.
[22] H. Xie, X. Wu, Z. Peng, Proc. 4th International Conference on Properties and Applications of Dielectric Materials, Brisbane, Australia, **1994**, p. 39.
[23] J. P. Perdew, R. G. Parr, M. Levy, J. L. Balduz, *Phys. Rev. Lett*. **1982**, *49*, 1691.
[24] L. Hedin, *Phys. Rev*. **1965**, *139*, A796.
[25] M. S. Hybertsen, S. G. Louie, *Phys. Rev. B* **1986**, *34*, 5390.
[26] C. Adamo, V. Barone, *J. Chem. Phys*. **1999**, *110*, 6158.
[27] L. Chen, H. D. Tran, C. Wang, R. Ramprasad, *J. Chem. Phys*. **2015**, *143*, 124907.

© 2017 WILEY-VCH Verlag GmbH & Co. KGaA, Weinheim